

## Dispersion of Magnetic Excitations in the Cuprate $\text{La}_2\text{CuO}_4$ and $\text{CaCuO}_2$ Compounds Measured Using Resonant X-Ray Scattering

L. Braicovich,<sup>1</sup> L. J. P. Ament,<sup>2</sup> V. Bisogni,<sup>3</sup> F. Forte,<sup>2,4</sup> C. Aruta,<sup>5</sup> G. Balestrino,<sup>6</sup> N. B. Brookes,<sup>3</sup> G. M. De Luca,<sup>5</sup> P. G. Medaglia,<sup>6</sup> F. Miletto Granozio,<sup>5</sup> M. Radovic,<sup>5</sup> M. Salluzzo,<sup>5</sup> J. van den Brink,<sup>2,7</sup> and G. Ghiringhelli<sup>1</sup>

<sup>1</sup>*CNR-INFM Coherentia and Soft, Dipartimento di Fisica, Politecnico di Milano, I-20133 Milano, Italy*

<sup>2</sup>*Institute-Lorentz for Theoretical Physics, Universiteit Leiden, NL-2300 RA Leiden, The Netherlands*

<sup>3</sup>*European Synchrotron Radiation Facility, Boîte Postale 220, F-38043 Grenoble, France*

<sup>4</sup>*CNR-INFM SuperMat, Dipartimento di Fisica, "E.R. Caianiello", Università di Salerno, I-84081 Baronissi, Italy*

<sup>5</sup>*CNR-INFM Coherentia, Dipartimento Scienze Fisiche, Università di Napoli "Federico II", I-80126 Napoli, Italy*

<sup>6</sup>*CNR-INFM Coherentia and Dipartimento di Ingegneria Meccanica, Università di Roma Tor Vergata, I-00133 Roma, Italy*

<sup>7</sup>*Institute for Molecules & Materials, Radboud Universiteit Nijmegen, NL-6500 GL Nijmegen, The Netherlands*

(Received 22 September 2008; published 20 April 2009)

By resonant inelastic x-ray scattering in the soft x-ray regime we probe the dynamical multiple-spin correlations in the antiferromagnetic cuprates  $\text{La}_2\text{CuO}_4$  and  $\text{CaCuO}_2$ . High resolution measurements at the copper  $L_3$  edge allow the clear observation of dispersing bimagnon excitations. Theory based on the ultrashort core-hole lifetime expansion fits the data on these coherent spin excitations without free parameters.

DOI: 10.1103/PhysRevLett.102.167401

PACS numbers: 74.25.Ha, 74.72.-h, 75.25.+z, 78.70.Ck

In the early days of high temperature superconductivity it was already recognized that the magnetic properties of these materials were intimately related to the superconducting ones. When doped, the long-range ordered antiferromagnetic background of pristine copper oxide insulators gets frustrated leading to short range antiferromagnetic fluctuations and superconductivity. That is why the magnetic properties of parent compounds have attracted so much attention since the discovery of superconductivity in cuprates. The spin dynamics of cuprates has been studied mostly with neutron inelastic scattering [1–3] that, up to now, has provided momentum resolved information only on single spin-flip processes (magnons), although it is known that multiple magnons also produce a broad spectral contribution [4–6]. As in cuprates the interatomic exchange interaction  $J$  is  $\sim 100$  meV; multiple-magnon excitations lie in energy range (100–500 meV) where, up to now, both neutron and x-ray experiments have been limited by technical obstacles. Nevertheless resonant inelastic x-ray scattering (RIXS) has the potential to probe very effectively the dynamics of two spin flips [7,8], so that one can directly observe the dispersion of bimagnon excitations, which are coherent states of two magnons [9]. This is far beyond the capabilities of traditional low energy optical techniques [10–12], which are constrained to zero momentum transfer.

Following the first theoretical suggestions of Refs. [13,14], partly confirmed at the oxygen  $K$  edge by Harada [15] and co-workers, Hill *et al.* [16] have recently found that Cu  $K$  edge RIXS spectra of undoped antiferromagnetic cuprates at 20 K show a sizable peak around 500 meV when the transferred momentum  $\mathbf{q}$  corresponds to the  $(\pi, 0)$  point of the reciprocal space. This feature, suppressed by doping, has been assigned to the simulta-

neous excitation of two magnons. This finding has boosted important theoretical work on the determination of bimagnon dispersion in cuprates by Cu  $K$  edge RIXS [7,8,17–19]. In this Letter we show that Cu  $L_3$  RIXS is an ideal technique to determine bimagnon dispersion in cuprates. In  $\text{La}_2\text{CuO}_4$  and  $\text{CaCuO}_2$  we have found dispersing spectral features both at room temperature and at 30 K. Along the  $(0, 0) \rightarrow (\pi, 0)$  direction their peak position ranges from  $\sim 0$  in  $(0, 0)$  to 400 meV at  $(\sim \frac{2\pi}{3}, 0)$ . Given the energy scale and the theoretical predictions, we assign these dispersing features to bimagnon excitations.

The RIXS process at the copper  $L_3$  edge of cuprates begins with the absorption of an x-ray photon, resonantly promoting an electron from the inner Cu  $2p$  state to its  $3d$  valence shell; see Fig. 1(a). As in the undoped cuprates Cu is basically in a  $3d^9$  configuration, the x-ray photon absorption produces a  $2p^6 3d^9 \rightarrow 2p^5 3d^{10}$  exciton. The second step is the decay of the intermediate state,  $2p^5 3d^{10} \rightarrow 2p^6 3d^{9*}$ , which leaves the material behind in an excited state indicated by the  $*$ , and produces outgoing photons of which we measure energy and momentum. Whereas in the initial and final state a spin  $\frac{1}{2}$  is present in the copper  $3d$  shell, in the  $2p^5 3d^{10}$  intermediate state the  $3d$  shell is completely filled, having no spin at all, and, due to the strong spin-orbit interaction, for the  $2p$  hole spin is not a good quantum number. So in Cu  $L_3$  edge RIXS ( $2p_{3/2}$  core hole) a nonmagnetic impurity is introduced in the intermediate state. This impurity is dynamically screened by the rest of the system, inducing spin reorientations at sites around it [7,8]. Besides these spin excitations the RIXS spectra also show, at higher energies, intense  $dd$  excitations that are due to the redistribution of electrons within the copper  $3d$  shell [20,21], possibly accompanied by spin-flip excitations as well [22,23].

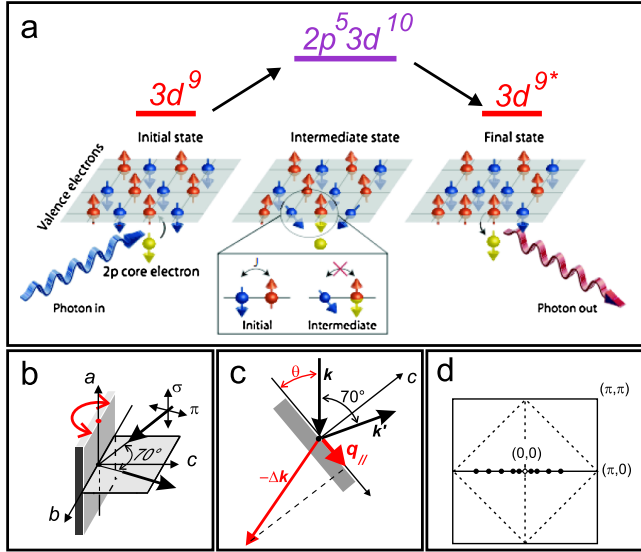


FIG. 1 (color online). The  $L_{2,3}$  edge RIXS process and the experimental geometry. (a) Schematic representation of the resonant scattering leading to a bimagnon; the actual spin alignment direction does not matter in the proposed scattering mechanism as long as an antiferromagnetic interaction is present. (b) The experimental scattering geometry, where the scattering angle is fixed at  $110^\circ$  ( $70^\circ$  back scattering) and the sample can be rotated around its  $a$  axis. (c) determination of  $q_{\parallel}(\theta)$ , projection onto the  $ab$  plane of the  $\Delta\mathbf{k}$  momentum lost by the scattering photons. Panel (d) Points in the reciprocal space corresponding to the spectra measured for  $\theta = 10^\circ \rightarrow 90^\circ$ .

The measurements were done at the European Synchrotron Radiation Facility in Grenoble (ID08 beam line and AXES spectrometer [24]), with linearly polarized x rays, either perpendicular ( $\sigma$ ) or parallel ( $\pi$ ) to the scattering plane containing the sample  $c$  axis [Fig. 1(b)]. We used  $\text{CaCuO}_2$  (CCO) and  $\text{La}_2\text{CuO}_4$  (LCO) thin films (100 nm) grown by pulsed laser deposition on (001)  $\text{LaAlO}_3$  and  $\text{SrTiO}_3$ , respectively [25]. The surface was not treated after insertion in the measurement vacuum chamber as L-RIXS probes hundreds of nm under the surface. No sample degradation was seen during the measurements. The spectra were measured at room temperature and some selected LCO cases at 30 K. The scattering angle was  $110^\circ$  ( $70^\circ$  backscattering) and by rotating the sample we varied the transferred momentum  $q_{\parallel}$  along the  $(0, 0) \rightarrow (\pi, 0)$  direction in the two-dimensional crystallographic Brillouin zone [see Fig. 1(c)]: for  $\theta = 10^\circ \rightarrow 55^\circ \rightarrow 90^\circ$  we spanned  $q_{\parallel} = -2.1 \rightarrow 0 \rightarrow 1.7$ . Every spectrum was measured at fixed incident photon energy (Cu  $L_3$  absorption peak at around  $\sim 931$  eV). The monochromator before the sample and the spectrometer contributed almost equally to the total energy resolution of  $\sim 400$  meV. One spectrum required about 80 min with  $\sim 1600$  and  $\sim 400$  photon counts on the  $dd$  and low energy peaks (one data point every 72 meV). Both CCO and LCO are undoped, antiferromagnetic layered cuprates. CCO is also called “infinite layer” for being constituted by only

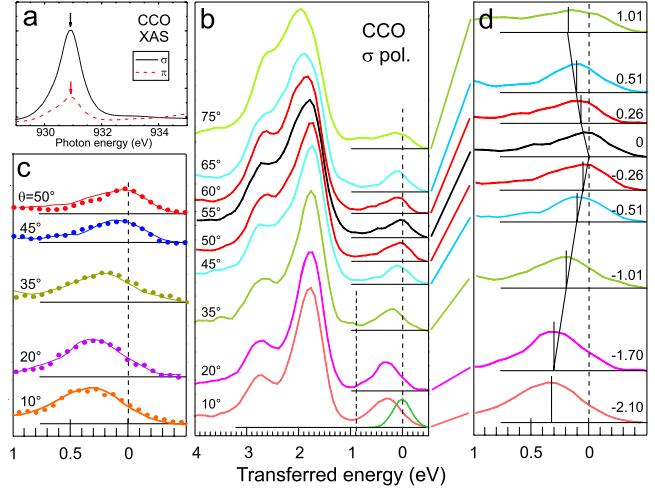


FIG. 2 (color online). Experimental results of  $\text{CaCuO}_2$  (a) Cu  $L_3$  x-ray absorption spectrum (XAS), the vertical lines indicate the excitation energy. (b) CCO RIXS spectra for various incidence angles  $\theta$  with  $\sigma$  polarization: the  $dd$  excitations ( $E = 1.5\text{--}3$  eV) evolve in shape but do not disperse, whereas the low energy feature below 1 eV disperse versus  $q_{\parallel}$ , as highlighted in (d), where the value of  $q_{\parallel}$  is indicated. In (c) the  $\pi$  (circles) and  $\sigma$  (lines) cases are compared after normalization to the  $dd$  peak, which is almost equivalent to scaling to the absorption cross section.

$\text{CuO}_2$  sheets separated by  $\text{Ca}^{2+}$  spacers, with no apical oxygens. LCO is the parent compound of  $\text{La}_{2-x}\text{Sr}_x\text{CuO}_4$  high  $T_c$  superconductors. The spin  $\frac{1}{2}$  at the Cu sites lie in the  $ab$  plane in both cases. Reported Néel temperatures of CCO and LCO are 537 and 325 K, respectively, [3,26]. We used thin films because their  $ab$  surface is very flat and stable and their orientation is easy to control; moreover CCO is not available as bulk single crystal.

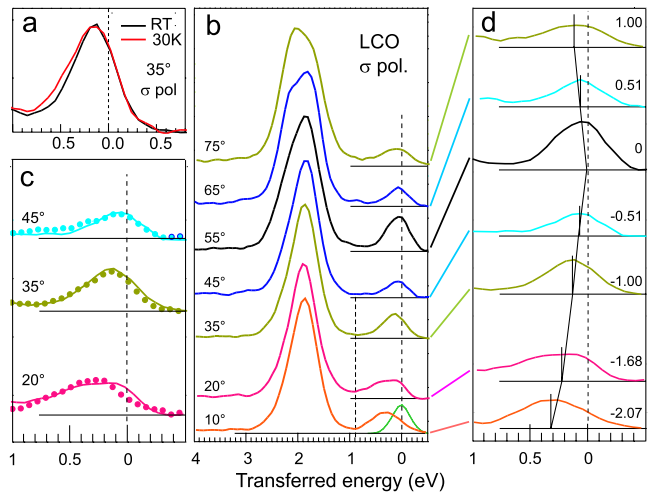


FIG. 3 (color online). Experimental results of  $\text{La}_2\text{CuO}_4$ . In (a) the low energy feature with  $\theta = 35^\circ$  ( $q_{\parallel} = 1.03$ ) measured at room  $T$  and 30 K are compared. In (b), (c), and (d) same as in Fig. 2.

Figures 2 and 3 show the experimental spectra for CCO and LCO. The spectra are dominated by  $dd$  excitations from 1.5 to 3 eV, in agreement with previous results [21,27,28]. The cross section of the various  $dd$  excitations changes with  $\theta$  as expected from crystal field model calculations [21,23]. The  $dd$  spectra of CCO and LCO are different: CCO has no apical oxygen, so the tetragonal distortion is much stronger than in LCO, leading to a more extended energy scale. Below we will concentrate on the  $E < 1$  eV spectral region. Figures 2(d) and 3(d) show how the low energy feature evolves with  $q_{\parallel}$  in the two samples. The peak position changes symmetrically to  $q_{\parallel} = 0$  reaching  $\sim 400$  meV for  $q_{\parallel} \approx \frac{2\pi}{3}$ . The first key result is that this feature is present, with similar intensity and energy, in the two samples and for both  $\sigma$  and  $\pi$  polarizations. Given the very different  $dd$  excitation spectra in the two samples contrasting the similarity of the low energy feature, the latter cannot be assigned to crystal field ( $dd$ ) excitations. The second key result is its strong dispersion, indicating unambiguously its wavelike nature. Moreover we emphasize the different behavior of the  $dd$  and low energy features: the former evolves rather monotonically with  $\theta = 10^\circ \rightarrow 90^\circ$ , whereas, the latter follows a dispersion symmetric with respect to  $\theta = 55^\circ$ , i.e.,  $q_{\parallel} = 0$ . Thus, already from the raw data it seems reasonable to assign it mainly to bimagnon excitations.

In order to better compare these experimental results to theory, a careful treatment of the spectra is needed (Fig. 4). First we need to subtract the elastic peak from the spectra. The red curve is an analytical fitting of the measured elastic peak, whose intensity is tuned to the measured spectrum. The relative positions of the spectrum and of the elastic peak is determined experimentally by taking, for each spectrum, an off-resonance spectrum on an Ag paint strip at the same excitation energy used for RIXS. The difference spectrum is the inelastic contribution, and the position of the bimagnon peak is defined in correspondence of its maximum intensity. These results can thus be compared with the corresponding quantity obtained from the theoretical spectral function (the lifetime broadening is already included in the theory and a Gaussian convolution is sufficient to account for the experimental resolution). The position of the maximum is rather well-defined, but with the present resolution it is premature to discuss the spectral shape. The robustness of the values of the bimagnon peak energy has been tested by exploring different positions and intensities of the elastic peak within the experimental uncertainties and noise. This procedure led to the error bars in the bimagnon energy displayed in Figs. 4(b) and 4(c). At the  $L_3$  resonance, cuprates are favorable because the elastic peak is weak and its subtraction is safe; we can detect features down to  $\sim 120$  meV. The bimagnon feature is basically independent of photon polarization when the spectra are normalized to the absorption coefficient, i.e., to the number of core holes created in the intermediate state. On their way out of the

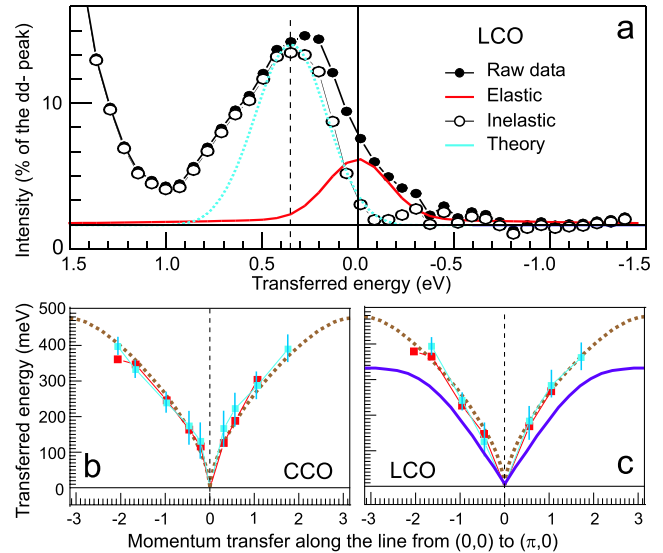


FIG. 4 (color online). Data treatment and summary of dispersion results. In (a) the LCO spectrum at  $\theta = 35^\circ$ ,  $\sigma$  polarization: from raw data (full circles) the experimental elastic peak (red line) is subtracted, giving the inelastic spectrum (open circles) to be compared with theoretical spectral shape (light blue line). In (b) and (c) the low energy feature peak position is plotted vs  $q_{\parallel}$  (experiment: red squares for  $\sigma$ , blue squares with error bars for  $\pi$ ). In (c) also the one magnon dispersion (purple line) from Ref. [3] is shown. Brown lines correspond to theoretical dispersion calculated with  $J = 120$  meV [3], and accounting for the experimental resolution.

sample scattered photons can be resonantly reabsorbed so that the peak of the low energy feature can be displaced to higher energy loss. The measurements up to ( $\theta \leq 75^\circ$ ) can be used safely because the dispersion is symmetric in  $q$  and  $-q$  in spite of the different self-absorption which is very much dependent on the angle. This shows that the self-absorption effect is marginal. The XAS were measured both with the drain current [Fig. 2(a)] and with total fluorescence; the  $L_3$  peak position interesting to us is the same in the two cases.

The bimagnon origin of the dispersing low energy feature is supported by comparing the data to theory. In the context of  $K$  edge RIXS on Mott insulators we have previously developed the microscopic theory [7,8] for multiple-magnon scattering that results from the sudden change of the superexchange magnetic interaction in the intermediate state, relying on the so-called ultrashort core-hole lifetime (UCL) expansion [29]. It follows from elementary considerations that the theoretical descriptions of resonant scattering at the  $L$  and  $K$  edge are equivalent in leading order of the UCL expansion. This allows the direct comparison of the experimental and theoretical bimagnon dispersions shown in Fig. 4. The agreement is excellent both for CCO and LCO, in particular, when considering that our theory contains only one parameter, the antiferromagnetic nearest neighbor exchange coupling  $J = 120$  meV, which we take from neutron measurements on

LCO [3], so that the fit contains no free parameters. The same  $J$  could be used to fit CCO data within the error bars. Although a full comparison of magnetic RIXS at the  $L$  and  $K$  edge cannot be made here, we mention two major differences. At the  $L$  edge the core-hole lifetime is longer and, at the same time, the  $2p^5 3d^{10}$  intermediate configuration produces a slightly stronger magnetic perturbation because it completely blocks all magnetic exchange paths involving the site with the core hole. These two factors work together in enhancing scattering terms that are second order in the UCL expansion. This higher order contribution should become particularly visible close to  $q_{\parallel} = 0$ , where the first order term produces no scattering. This  $q_{\parallel} = 0$  second order bimagnon contribution is computed to have a very broad maximum around  $E = 4.2J$ . The experimental spectra show indeed some intensity around 500 meV at  $q_{\parallel} = 0$  but a definitive assignment of this spectral weight as a second order contribution requires higher resolution data.

The experimental dispersion summarized in Figs. 4(b) and 4(c) is clearly incompatible with the assignment of the low energy feature to single magnons: already at  $(\frac{2\pi}{3}, 0)$  in both samples energy  $E \approx 400$  meV exceeds the 315 meV found at  $(\pi, 0)$  in inelastic neutron scattering data of LCO [3]. On the contrary, for LCO in optical absorption (OA) and Raman spectroscopy peaks at  $E \approx 400$  meV have been assigned to bimagnons (plus phonon for OA) [10,30]. And  $K$  edge RIXS results [16] look compatible with our data: at  $(\pi, 0)$  the peak found at  $\sim 500$  meV was assigned to bimagnons. The difference between optical and x-ray results can possibly be due to differences in double spin wave excitation. In our theory the magnon-magnon interaction is for the moment neglected. When the relative momentum of the two magnons is small, which is the case when also  $\mathbf{q}$  is small, interaction effects are small in general. At higher energy transfer closer to the edge of the Brillouin zone, they cause a moderate redshift of the main peak [17,18] which is within the present experimental resolution. In addition in our data we found that temperature has little influence on bimagnons [Fig. 3(a)]: at 30 and 300 K the peak is at the same energy but the high energy tail gets more expanded at low  $T$ ; this is in qualitative agreement with single magnon results [3] and shows that in RIXS phonons are basically decoupled from bimagnons. Finally it is not surprising that in CCO and LCO bimagnons are at almost identical energy: the measured Cu-O distance in the two films is very similar ( $a, b = 0.380$  nm for LCO,  $a, b = 0.384$  nm for CCO), thus leading to the same value for  $J$ .

In conclusion, by measuring the bimagnon dispersion we could access dynamical multiple-spin correlations in antiferromagnetic cuprates. Moreover, we have demonstrated that soft x-ray RIXS is becoming a very useful tool to measure magnetic excitations.  $L_3$  edge RIXS is complementary to neutron scattering and optical spectroscopy and widens the experimental palette in the study of

magnetic and charge modes of cuprates and other 3d transition metal compounds. It can be measured equally well on single crystals and thin films. Finally, x-ray scattering is also sensitive to electronic excitations: in doped cuprates  $L$  edge RIXS can be used to measure collective modes having both magnetic and charge character. Those experiments are potentially enlightening on the influence of the antiferromagnetic background on cuprate superconductivity.

We thank G.A. Sawatzky, M. van Veenendaal, and M. Grioni for very stimulating discussions. The measurements were taken under the AXES contract between the ESRF and the INFN/CNR.

- 
- [1] B. Vignolle *et al.*, Nature Phys. **3**, 163 (2007).
  - [2] S.M. Hayden *et al.*, Nature (London) **429**, 531 (2004).
  - [3] R. Coldea *et al.*, Phys. Rev. Lett. **86**, 5377 (2001).
  - [4] R.A. Cowley *et al.*, Phys. Rev. Lett. **23**, 86 (1969).
  - [5] J. Lorenzana *et al.*, Phys. Rev. B **72**, 224511 (2005).
  - [6] N.B. Christensen *et al.*, Proc. Natl. Acad. Sci. U.S.A. **104**, 15 264 (2007).
  - [7] J. van den Brink, Europhys. Lett. **80**, 47003 (2007).
  - [8] F. Forte *et al.*, Phys. Rev. B **77**, 134428 (2008).
  - [9] J. Lorenzana and G.A. Sawatzky, Phys. Rev. Lett. **74**, 1867 (1995).
  - [10] J.D. Perkins *et al.*, Phys. Rev. B **58**, 9390 (1998) and references therein.
  - [11] G. Blumberg *et al.*, Science **278**, 1427 (1997).
  - [12] T.P. Devereaux and R. Hackl, Rev. Mod. Phys. **79**, 175 (2007) and references therein.
  - [13] K. Tsutsui *et al.*, Phys. Rev. Lett. **83**, 3705 (1999).
  - [14] K. Okada and A. Kotani, J. Phys. Soc. Jpn. **69**, 3100 (2000).
  - [15] Y. Harada *et al.*, Phys. Rev. B **66**, 165104 (2002).
  - [16] J.P. Hill *et al.*, Phys. Rev. Lett. **100**, 097001 (2008).
  - [17] T. Nagao and J.I. Igarashi, Phys. Rev. B **75**, 214414 (2007).
  - [18] F.H. Vernay *et al.*, Phys. Rev. B **75**, 020403(R) (2007).
  - [19] A. Donkov and A.V. Chubukov, Phys. Rev. B **75**, 024417 (2007).
  - [20] P. Kuiper *et al.*, Phys. Rev. Lett. **80**, 5204 (1998).
  - [21] G. Ghiringhelli *et al.*, Phys. Rev. Lett. **92**, 117406 (2004).
  - [22] G. Ghiringhelli *et al.*, J. Phys. Condens. Matter **17**, 5397 (2005).
  - [23] M.A. van Veenendaal, Phys. Rev. Lett. **96**, 117404 (2006).
  - [24] M.E. Dinardo *et al.*, Nucl. Instrum. Methods Phys. Res., Sect. A **570**, 176 (2007).
  - [25] G. Balestrino *et al.*, J. Mater. Chem. **5**, 1879 (1995).
  - [26] D. Vaknin *et al.*, Phys. Rev. B **39**, 9122 (1989).
  - [27] L.-C. Duda *et al.*, J. Electron Spectrosc. Relat. Phenom. **110–111**, 275 (2000).
  - [28] G. Ghiringhelli *et al.*, Phys. Rev. B **76**, 085116 (2007).
  - [29] J. van den Brink and M. van Veenendaal, Europhys. Lett. **73**, 121 (2006).
  - [30] S. Sugai *et al.*, Phys. Rev. B **42**, 1045 (1990).